On Dual Actuation in Atomic Force Microscopes

Khalid El Rifai, Osamah El Rifai, and Kamal Youcef-Toumi
77 Massachusetts Ave. Room 3-348, Cambridge, MA 02139
elrifai@mit.edu,osamah@mit.edu, youcef@mit.edu

Abstract

In this paper, a solution to the control problem of dual actuation in atomic force microscopes (AFMs) is presented. The use of two actuators to balance the trade-off between bandwidth, range, and precision has been recently extended to nano-positioning systems. Despite existing demands, this concept undergoes fundamental limitations towards its extension to AFMs. This is attributed to the non-conventional requirement imposed on the control signal response, as it used to create the image of the characterized surface.

keywords: AFM control, imaging, nano- systems, dual actuator.

1 Introduction

The atomic force microscope (AFM) has become a very popular tool in research and industries of Nanotechnology, Bio-technology, MEMS, and life sciences. The AFM has been primarily actuated by piezoelectric tube actuators. However, the system bandwidth has been found to be significantly lower than the actuator's open loop resonance. This has limited AFM's use as an inspection tool in industry and in real-time monitoring of fast microscopic processes such as biological processes. PID controllers are commonly used in AFM systems to facilitate user tuning of the controllers for different sample-probe combinations. More recently, H_∞ synthesis has been used [4] to design a controller based on an experimentally identified model of the piezotube dynamics. As reported by the authors, their control implementation lead to five times faster scanning speed than obtained using a PID controller. However, this was at the expense of the control signal containing significant oscillations not due to the scanned sample. As the control signal is used to create the image of the scanned surface, the image was not recordable.

Meanwhile, a piezoelectric film has been patterned onto cantilevers, see for example [**?**], allowing for an alternate actuation scheme. The use of self-actuated microcantilevers has been found to offer bandwidth enhancements yet at the expense of a small allowable travel range. These results suggested use of dual actuation as a natural solution. In this context, a thermal actuator in [5] and a piezotube in [6] have been combined with a piezoelectric cantilever to scan a selected sample. In these efforts, it has been demonstrated that range beyond that of the fine actuator can be achieved via the additional actuator. However, the important question of whether an improvement in the dynamic performance, and thus throughput, would be achieved with dual actuation over single actuation has not been answered. This paper aims to answer this question, which does not follow the standard dual actuator formulation, due to the unique objective on the control signal in AFMs.

2 AFM Systems

The basic principle of the AFM operation is based on using a micro-cantilever with a sharp object at its tip to probe a scanned surface. The cantilever is mounted on a piezoelectric tube scanner, which can translate both laterally and vertically, see Figure 1. Lateral scanning is performed via the piezotube actuator with a prescribed scan size and rate. As the probe touches a feature on a surface, it generates a force causing the cantilever to deflect. Therefore, light from a laser source reflects off the cantilever's tip and the corresponding change in cantilever deflection is recorded via a position sensitive split photodetector (PSD). This sensor measurement is then compared to a chosen setpoint detector voltage, reflecting a nominal setpoint cantilever deflection. The difference between the current sensor output and nominal output is then sent to a controller. The controller causes a piezoelectric actuator to extend or retract via an input voltage in order to maintain the nominal detector setpoint. This actuator is either the piezotube actuator or the self-actuated piezocantilever. This is referred to as contact mode AFM. Whereas, tapping mode AFM is similarly operated but rather with intermittent contact with the sample. This is achieved by driving the cantilever through a harmonic excitation near its

resonant frequency. In this case, piezoelectric actuation is used to maintain a constant root-mean-square (RMS) cantilever deflection.

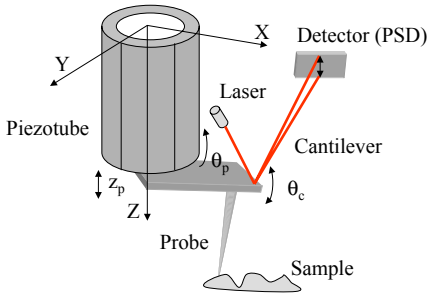

Figure 1: Principle of AFM operation.

3 AFM Dynamical Model

In this section, we extend our earlier model to span the dual actuation configuration. A brief explanation of the model will follow, for details see [1, 2, 3]. The system's dynamics of interest are characterized by three degrees-of-freedom: z_p the extension of the piezotube, θ_p the piezotube bending, about the Y-axis in Figure 1, and θ_c the cantilever bending relative to the tube base. These are the only degrees-of-freedom of interest in terms of the vertical dynamics. In AFMs, the control action is concerned with the vertical and not the lateral dynamics of the scanner. The lateral motion, i.e., the scanning, is prescribed by the choice of the scanned spot size and the sampling resolution via open loop input voltages. Though it is desired that the tube only extends or retracts to a given voltage, this ideal behavior is not achieved in practice. A small piezotube bending in response to this input voltage is usually observed due to inevitable tube eccentricity. Therefore, it is necessary to include the bending of the tube θ_p as it is observable at the output. Coupling between extension and bending dynamics of piezotube scanners used in AFMs was first reported in [1]. Equations (1-4), govern the system dynamics of interest. Here, the first three equations describe the dynamics of each DOF and the fourth equation is the measurement. Where i^*, j^*, and m^* are the number of modes considered for each degree-of-freedom, ζ is damping ratio, and ω is natural frequency.

$$\theta_p(s) \approx \sum_{j=1}^{j^*} \frac{k_{\theta pj}}{s^2 + 2\zeta_{\theta p_j}\omega_{\theta p_j} s + \omega^2_{\theta p_j}} u_1 \quad (1)$$

$$z_p(s) \approx \sum_{m=1}^{m^*} \frac{k_{z_p m}}{s^2 + 2\zeta_{z_p m}\omega_{z_p m} s + \omega^2_{z_p m}} u_1 \quad (2)$$

$$\begin{aligned} \theta_c(s) \approx & \sum_{i=1}^{i^*} \frac{(a_{2zi}s^2 + a_{1zi}s)}{s^2 + 2\zeta_{ci}\omega_{ci}s + \omega^2_{ci}} z_p \\ & + \frac{(a_{2\theta i}s^2 + a_{1\theta i}s)}{s^2 + 2\zeta_{ci}\omega_{ci}s + \omega^2_{ci}} \theta_p \\ & + \frac{a_{fi}}{s^2 + 2\zeta_{ci}\omega_{ci}s + \omega^2_{ci}} f_c \\ & + \frac{k_{\theta ci}}{s^2 + 2\zeta_{ci}\omega_{ci}s + \omega^2_{ci}} u_2 \\ & + \frac{k_{\theta ci}}{s^2 + 2\zeta_{ci}\omega_{ci}s + \omega^2_{ci}} f_h \end{aligned} \quad (3)$$

$$y_m = \theta_p + \theta_c \quad (4)$$

External inputs u_1 and u_2 are input voltages applied to the piezotube and piezocantilever,respectively. In Equation (3), f_h is a harmonic excitation used in tapping mode AFM to drive the cantilever near it's 1^{st} resonance. Whereas, f_c is the probe-surface interaction force. This probe-sample force is a nonlinear function of the relative position between the probe and the contacted surface. The following approximation of the probe-surface force will be used, where c_1 and c_2 are constants:

$$f_c \approx c_1\theta_p + c_2 z_p + d \quad (5)$$

In this regard, the 1^{st} order terms in the contact force (in contact mode) or the averaged probe-surface interaction force (in tapping mode) are retained, see Equation (5). Whereas, deviations from this nominal force, including any nonlinearities, will be represented as an external disturbance d. This disturbance accounts for changing the cantilever's deflection during scanning. The following relation between the detector output y_m, input voltages u_1 and u_2, the harmonic excitation f_h, and the topography induced disturbance d may be deduced from Equations (1-5):

$$y_m = P_1 u_1 + P_2(u_2 + f_h) + W_d d \quad (6)$$

Where $P_1(s)$, $P_2(s)$, and $W_d(s)$ are appropriate transfer functions, which depend on the number of modes included from each degree-of-freedom.

$P_1(s)$ is a $2(i^* + j^* + m^*)^{th}$ order transfer function with relative degree two. The poles are those corresponding to all of included modes. Whereas, $P_2(s)$ and $W_d(s)$ are transfer functions of order $2i^*$ of relative degree two. In here, the poles are those of the cantilever bending modes. Experimental frequency response results of AFM dynamics have been reported in earlier efforts [**?**, **?**, **?**]. Typical values of piezotube bending, piezotube extension, and cantilever bending 1^{st} resonances are of the order of few hundred Hz, few kHz, and tens of kHz, respectively.

4 AFM Control Problem

4.1 System Set-Up

The task of AFM control system in contact (or tapping) mode is to reject the effect of variations in the scanned surface on maintaining probe-surface contact (or intermittent contact). This is verified by maintaining a constant setpoint detector output (or constant RMS detector output). The height of the contacted surface at each scanned point is given by the product of the control voltage sent to the actuator at this point and the calibrated sensitivity of the actuator in nm/volts. In dual actuation, each control voltage is scaled by the corresponding actuator's sensitivity and the sum is used as an image.

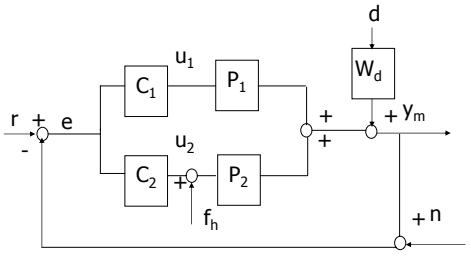

Figure 2: Block diagram of AFM dual actuator configuration.

Figure 3 shows the two signals of interest recorded during a selected AFM scan. The scan is made for a triangular silicon grating with an included angle of about 70°. Figure 3(a) shows the sample's height along a scanned cross section, i.e., the control signal scaled by the actuator's voltage-displacement sensitivity. In addition, the deflection signal, the difference between the detector's output and the setpoint output, is given in Figure 3(b). In the figure below two signals are shown for trace and retrace scans, which closely overlap in height data, Figure 2 (a), and are mirror images with respect to the horizontal for error in Figure 2 (b).

The block diagram representing the dual actuator AFM system is given by Figure 3. In this scenario, the piezotube and a piezocantilever are supplied with input voltages u_1 and u_2, respectively. The control action associated with each actuator input is represented by the controller transfer functions $C_1(s)$ and $C_2(s)$. Here, it is desired to maintain the output of the detector, y_m, at the nominal setpoint voltage, r or correspondingly the RMS value in tapping mode. In the block diagram, n represents measurement noise for the PSD sensor.

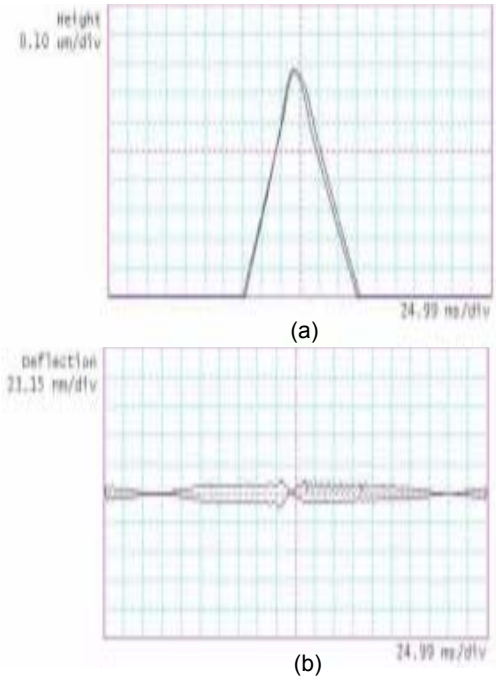

Figure 3: Experimental AFM signals: (a) control (height) signal, (b) error (deflection) signal.

4.2 Feedback Structural Limitations

The response of the control (image) and error (deflection) signals to the scanned surface variations, i.e., output disturbance, is governed by the control sensitivity S_u and the output sensitivity S_o functions, respectively. In feedback systems, the control and

output sensitivity functions are defined as follows:

$$S_u = \frac{u}{-d} \quad , \quad S_o = \frac{e}{-d} \tag{7}$$

Naturally the sensitivity function, S_o, is desired to be of a small gain at low frequencies up to a maximal possible bandwidth for good disturbance rejection. However, in AFMs an additional requirement is imposed on the control response. It is desired that the frequency response of the control sensitivity function contains no peaks within or near its bandwidth as well as rolls-off well before frequencies where noise is dominant. This leads to the control signal being representative of the disturbance created by the scanned sample's topography. This is required because the control signal is used to create the image of the scanned surface. If this is simultaneously achieved with the small error requirement on S_o, an accurate image of the scanned surface is recorded since the system is a regulator. However, these objectives are coupled, with the coupling taking the following form in single and dual actuation, respectively:

$$S_o = W_d - PS_u \tag{8}$$

$$S_o = W_d - P_1 S_{u1} - P_2 S_{u2} \tag{9}$$

This naturally suggests that for good disturbance rejection, $S_u \approx P^{-1}W_d$ within the frequency range of operation. In fact, resonances in the product $P^{-1}W_d$ become resonances in the control sensitivity's response. The 1^{st} resonance in this product for piezotube actuated AFM's is piezotube bending mode zeros, which are typically lightly damped of damping ratios of the order of 0.1 and of frequency of 200 to 800 Hz, see [**?**]. This leads to degrading the control response via a large peak in $S_u = CS$, unless the controller gain is sufficiently small near this zero frequency. Figure 4 is a sample AFM scan showing an image corruption with control oscillations that are not due to the sample's topography. It is noteworthy that the image shown has been recorded at a scan rate of only 1 Hz using a PI controller.

In the dual actuation, the sum u_1+u_2 is responsible for rejecting the full disturbance. However, the challenge is that the piezotube bending zeros also lead to peaks in the control sensitivity of the piezocantilever S_{u2} due to the algebraic constraint in Equation (9). Therefore, using an arbitrary choice of controllers $C_1(s)$ and $C_2(s)$ such that S_{u2} is of a bandwidth not lower than that of these zeros, will lead to oscillations in the 2^{nd} control voltage u_2 and thus corrupt the image.

Observe that if S_{u2} is not of bandwidth higher than these zeros then no performance enhancement is gained from dual actuation over single actuation.

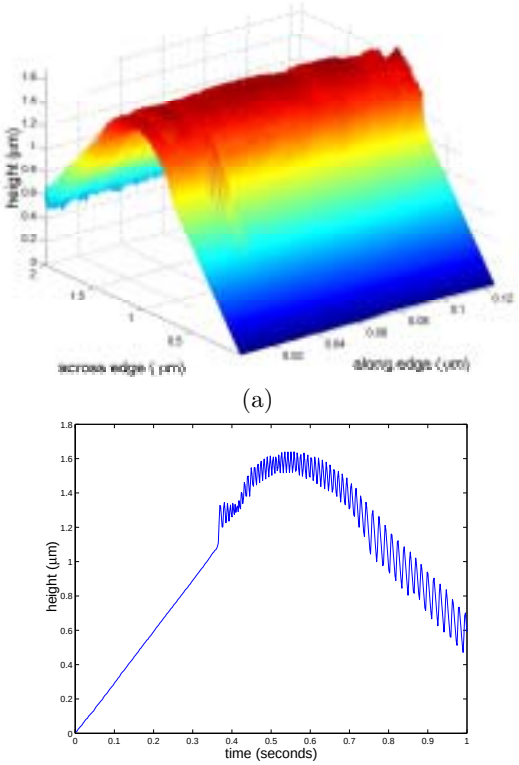

(a)

(b)

Figure 4: Experimental demonstration of image oscillations due to piezotube actuator dynamics (a) 3-D image, (b) cross section.

Therefore, in order for dual actuation to attain any performance improvement a careful controller design needs to be made. The proposed controller design takes advantage of the fact that plant dynamics canceled in the branch C_iP_i will not appear as a pole or a zero of the control sensitivity associated with the other controller. This is contrasted with the SISO situation, where inverting the dynamics automatically leads to control (image) oscillations due to the zeros. The proposed design can be made possible by choosing $C_1 \approx P_1^{-1}W_L$, where W_L is a low pass filter with bandwidth lower than that of the piezotube bending zero. Note that this requires that the controller commanding the piezotube needs to cancel the dynamics of the tube, within the bandwidth of operation of the piezocantilever, *after* rolling off before the 1^{st} zero. Therefore, the effect of these zeros on corrupting the control signal of the fast actuator is

removed. Note that this has been needed because the targeted feedback performance is to be achieved without corrupting the control signals, i.e., the image. If such a constraint were removed, then the problem can be trivially dealt with as any dual actuator problem.

5 Design Example

In this section, a sample experimentally identified model is used for controller design demonstration. Here, the 1^{st} piezotube bending resonance is at about 400 Hz and an anti-resonance at 550 Hz with damping ratios both approximately of 0.1. The 1^{st} extension mode resonance and anti-resonance are at 4.6 kHz and 3.5 kHz, respectively, with damping ratio of 0.1. Finally, the cantilever bending mode resonance is at 50 kHz with a damping ratio of about 0.05. In this regard, an H_∞ controller synthesis is used to demonstrate the limitation due to the zeros as well as the proposed dual actuator design.

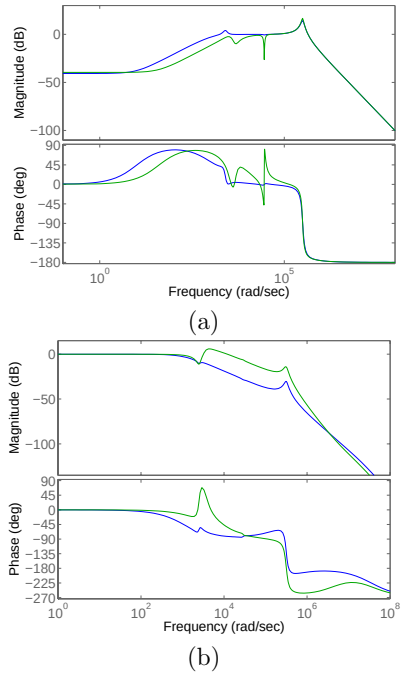

Figure 5: Bode diagrams for piezotube actuation : (a) sensitivity, (b) control sensitivity, where 'green' and 'blue' are for high and low bandwidth, respectively.

First, the single actuator, with a piezotube, system is considered. This is achieved by letting $u_2 = 0$ in Equation (6). Figure 5 shows the closed loop frequency response with an 8^{th} order controller, designed via an H_∞ synthesis. Here, a bandwidth of about $200Hz$ is achieved while maintaining an acceptable control response. Yet pushing the bandwidth further inevitably leads to a control sensitivity peak at about $6dB$, which is at $550Hz$ the frequency of the 1^{st} piezotube bending mode zero. This peak corresponds to an overshoot of about 20% in the control signal response to step change in the topography induced force disturbance. The step response of the control signal for both designs of Figure 5 are contrasted in Figure 7 (a). Such peaks in the control sensitivity are responsible for oscillations in the image as those in Figure 4. This example demonstrates the fact that the aforementioned limitation is independent of the control algorithm used as noted in [3].

Next, the dual actuated situation is contrasted with the piezotube actuated system. Here, the relative range of actuators is important. A typical design objective in a dual actuation scenario as this one is that S_{u1} would be of a large gain but low bandwidth. While for the fine actuator, S_{u2} is of lower gain but higher bandwidth. This is attributed to the fact that the input range available to the each actuator relative to the total size of the disturbance is different. In here, the ratio of S_{u1}/S_{u2} static gains will be designed to be about 5-6. This is in accordance with typical imaging ranges of $3-5\mu m$ for the piezotube and $.5-1\mu m$ for the piezocantilever. Note that the designed for ratio is a worst case scenario since it corresponds to minimal improvement due to the addition of the fast actuator. Obviously, if the maximal sample height is smaller then a bigger fraction of this disturbance is to be rejected by the fast actuator leading to better feedback bandwidth and disturbance rejection.

In Figure 6(b), the lower gain control sensitivity, S_{u2}, displays a flat response near the piezotube modes. This is made possible by use of controller C_1 that inverts all the dynamics of P_1 after rolling-off before the piezotube's 1^s zero, as detailed in section 4.2. Figure 7(b) shows the response of both control signals to a step change in the topography induced disturbance, which is clean unlike that in Figure 7(a) upon exceeding the zero. It is clear that the sum of a fast but small range signal (u_2) and a larger range but slower signal (u_1) add to one to cancel the unit step disturbance. In this situation, dual actuation can be used to improve over single actuation, which is measured by a reported improvement in bandwidth of three times. Otherwise, any gains in the feedback performance will be at the expense of image accuracy which is the goal of this system.

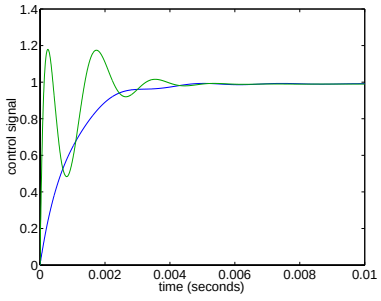

(a)

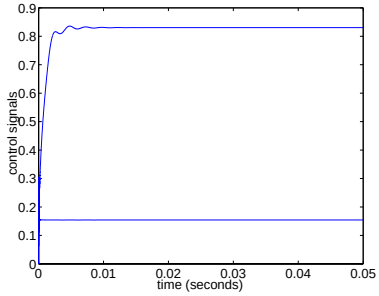

(b)

Figure 6: Control signal(s) response to a step disturbance for :(a) single actuation, where 'green' and 'blue' are for high and low bandwidth, respectively, (b) dual actuation

6 Conclusions

In this effort, the problem of dual actuation in AFMs has been addressed. The fact that the control signals are used to create the scanned surface's image introduces a novel challenge. This requires that both control signals used to actuate a piezotube and a piezocantilever need not to contain any oscillations not due to the scanned surface while enhancing feedback performance. It has been found that this cannot be achieved by an arbitrary choice of two controllers satisfying standard dual actuator objectives. A proposed design methodology has been provided and demonstrated with the estimated bandwidth improvement of at least three times.

References

[1] O. M. El Rifai, and K. Youcef-Toumi. Coupling in Piezoelectric Tube Scanners Used in Scanning Probe Microscopes, *American Control Conference*, Arlington, VA, pp.3251-3255, June 2001.

[2] O. M. El Rifai, and K. Youcef-Toumi. Dynamics of Contact-mode Atomic Force Microscopes, *American Control Conference*, Chicago, IL, pp.2118-2122, June 2000.

[3] O. M. El Rifai, and K. Youcef-Toumi. Trade-offs and Performance Limitations in Mechatronic Systems: A Case Study, *Annual Reviews in Control*, **2**, 2004.

[4] G.Schitter, P.Menold, H.F. Knapp, F.Allgower, and A.Stemmer. High Perfromance feedback for fast scanning atomic force microscopes. *Review of Scientific Instruments*, **72**(8), August 2001.

[5] T. Sulchek, S.C. Minne, J.D. Adams, D.A. Fletcher, A. Atalar, C.F. Quate, and D.M. Adderton. Dual integrated actautors for extended range high speed atomic force microscopy. *Applied Physics Letters*, **75**(11), September 1999.

[6] A. Egawa, N. Chiba, K. Homma, K. Chinone, and H. Muramatsu. High-speed scanning by dual feedback control in SNOM/AFM *Journal of Microscopy*, **194** , pp.325-328, May/June 1999.

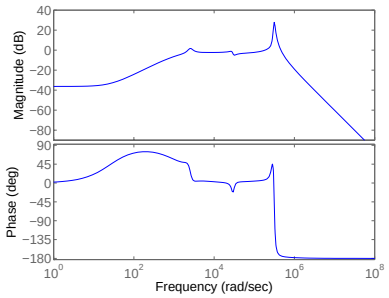

(a)

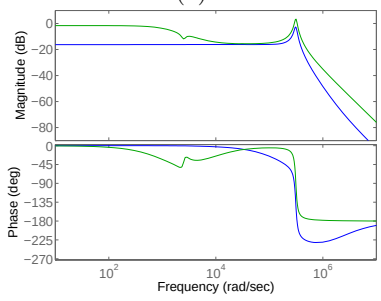

(b)

Figure 7: Bode diagrams for dual actuation : (a) sensitivity, (b) control sensitivity, where 'green' and 'blue' are for S_{u1} and S_{u2} , respectively.